Int. J. Electrochem. Sci., 9 **(2014)** 7325 - 7334

International Journal of
ELECTROCHEMICAL
SCIENCE
www.electrochemsci.org

Characterization of Corrosion Resistance in a Ferritic Stainless Steel Stabilized with Ti Addition

Ja young Hong[1], *Yong taek Shin*[2], *Hae Woo Lee*[1,*]

[1]Department of Materials Science and Engineering, Dong-A University, 840 Hadan-dong, Saha-gu, Busan 604-714, Republic of Korea
[2]Department of Ship Building and Marine Engineering, Dong-A University, 840 Hadan-dong, Saha-gu, Busan 604-714, Republic of Korea
[*]E-mail: hwlee@dau.ac.kr

Received: 24 July 2014 / *Accepted:* 25 August 2014 / *Published:* 29 September 2014

Ferrite stainless steel, with cheap prices and low thermal expansion coefficients due to no addition of nickel, is excellent in corrosion properties and high temperature corrosion resistance compared with cheap prices, widely used in automobile industry. However, intergranular corrosion and sensitization become problems. To prevent these problems, stabilizing elements are added to improve corrosion resistance. 3 kinds of welding wire, where adjusted Ti contents of a stabilizing element were added to AISI 436 stainless steel, to perform FCAW (Flux Cored Arc Welding) and thus to evaluate microstructures and corrosive properties. The specimen having no Ti additive was transformed into Ferrite + Martensite structure, while the specimen having Ti additives into fully ferrite structure. As Ti contents increased, the structure became refined. The evaluation of corrosive properties revealed that the addition of Ti allowed pitting potential to increase and passive region to widen. As Ti contents increased, the difference between pitting potentials was very slight, and pitting size and degree decreased.

Keywords: Ferritic stainless steel, welding, Titanium added, corrosion

1. INTRODUCTION

Recently emerging environmental issue and resource exhaustion require fuel efficiency improvement and life extension of automobiles. In this connection, the study of eco-environment materials development, high fuel efficiency, and exhaust gas purification has been actively performed in the automobile industry. [1] Especially, materials to satisfy heat resistance of the exhaust pipe, used at high temperature, have been developed. [2,3] As automobile exhaust pipe is close to the engine, it is exposed to high temperatures during the use. In the past, Si spheroidal graphite caset iron or steel

casting was widely used for automobile exhaust device materials. But cast iron and cast steel are lacking in heat resistance and difficult to reduce weight. In order to supplement disadvantages and satisfy heat resistance, the desired material could be used at over900℃ and should be light, satisfactory to both heat resistance and corrosion resistance. Thus, favored are stainless steels of long life and high temperature application. As stainless steel is capable of 40% lighter weight compared with cast iron or cast steel, and its thermal capacity is small, methane gas emissions can be reduced due to the temperature rise by catalyst. [4] Ferrite stainless steel, having lower thermal coefficient of expansion than austenite stainless steel, excellent in heat resistance and corrosion properties compared with lower price, is widely used for automobile parts. In particular, ferrite stainless steel 409L of a comparatively cheap price has been used but its high temperature corrosion properties limit the range of its use. [2,3,5,6] Among them, intergranular corrosion, which degrades corrosion resistance, strength, and flexibility, becomes the most serious problem. Intergranular corrosion occurs due to electrochemical potential differences between the base and the chromium deficient area as chromium, chrome carbide, and chrome carbonite are precipitating along grain boundaries. It is reported that Sigma phase and Kai Phase also cause intergranular corrosion. [3] Especially, as exhaust devices among automobile parts require high temperature strength and high temperature corrosion resistance, studies of material features and performances are actively being done. [7] To prevent the formation of intermetallic compounds and satisfy properties, contents of carbon or nitrogen are lowered, or ferrite stainless steel including stabilizing elements like Ti, Nb, Mo, etc. are being developed. It is reported that the addition of stabilizing elements have an positive influence on mechanical property as well as chemical stability. [8] Thus, addition of stabilizing elements and use of chrome welding materials help stabilize ferrite base, prevent sensitivity due to chrome carbide precipitation, and control microstructures. In this study, 3 kinds of specimen were prepared by controlling an alloy element of Ti content to 436 ferrite stainless steel flex core wire components, and heat treated for 2 hours at 850℃. And, through microstructure observation of the welded metal and potentiodynamic polarization test, corrosion features were evaluated.

2. EXPERIMENTAL PROCEDURE

2.1. Materials and welding

Test plate used in this study was 150 mm (length) x 200 mm (width) x 20 mm (thickness). Putting the same backing material as the welding material onto two contacting plates, flux-cored arc welding (FCAW) process was performed. Protective gas was 100% Ar. The shape of material was shown in Fig. 1, and welding conditions are in Table 1.

Also, The chemical composition of welded stainless steel was measured by an Optical Emission Spectrometer (Metal-LAB75/80J, GNR srl, Italy), and the result was shown in Table 2. The chemical compositions of welding rod were based on the AISI 436 stainless steel. And three types of the welding wire were made by modifying the Ti contents in the flux to analyze difference from

corrosion resistance. Test specimens were designated as No.1, No.2, No.3 respectively. Macrostructure was shown in Fig. 2.

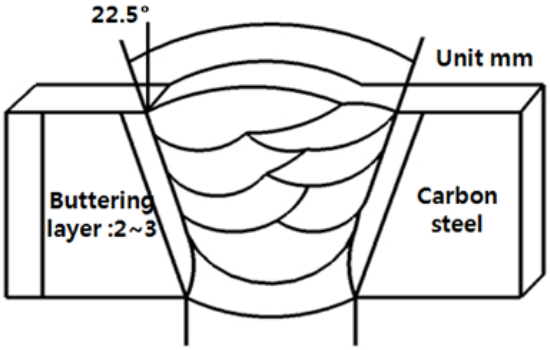

Figure 1. Schematic diagrams of weldment

Table 1. Welding parameters

Weld metal	Current (A)	Voltage (v)	Welding speed (cm/min)	Heat input (KJ/cm)	Interlayer temperature (℃)
436	150-300	24-33	20-60	14-15	150

Table 2. Chemical composition of weldmetals

As-weld metals	C	Si	Mn	P	S	Cr	Ni	Ti	Mo
No.1	0.02	0.4	0.5	0.008	0.007	16	0.01	free	0.9
No.2	0.02	0.4	0.5	0.008	0.007	16	0.01	0.5	0.9
No.3	0.02	0.4	0.5	0.008	0.007	16	0.01	0.8	0.9

2.2. Microstructure and Phase analysis

The specimens were etched after rough grinding and fine grinding. Etching solution - 60ml HNO_3, 40ml water – was used for ferrite stainless steel. To observe macro image and microstructure of specimens, scanning electron microscopy with an energy dispersive spectroscopy (SEM-EDS) (JSM-6700f, Jeol, Japan) detector was used. To analyze the Ti(C,N) and chrome carbides precipitation, crystal texture analysis was performed using the Electron Back Scatter Diffraction (EBSD).

2.3. Corrosion property test

Electrochemical test method of the specimens was a potentiodynamic method. Electrolyte used was 3.5% sodium chloride solution. The range of potential was set to from -1V to +1V, and scan rate

to 0.2 mV/s. Working electrodes for potentiodynamic polarization test were each specimen, a counter electrode was made of platinum foil, and a reference electrode was the silver-silver chloride electrode.

Figure 2. Macrostructure of specimen (a) No.1 (b) No.2 (c) No.3

2.4. Corrosion property test

Electrochemical test method of the specimens was a potentiodynamic method. Electrolyte used was 3.5% sodium chloride solution. The range of potential was set to from -1V to +1V, and scan rate to 0.2 mV/s. Working electrodes for potentiodynamic polarization test were each specimen, a counter electrode was made of platinum foil, and a reference electrode was the electrode of Ag-AgCl/KCl.

3. RESULTS AND DISCUSSION

3.1. Effects of chemical composition on microstructure

Fig. 2 shows the picture of macrostructure. As shown in the picture, we can identify visually that, as Ti content goes higher, the structure becomes finer. When Ti is added, TiN formed in liquid phase acts as a core into finer crystal grains, resulting in improvement of mechanical properties of welding part, said the report. In general, there are two kinds of condensation mode in ferrite stainless steel welding part: fully ferrite structure and ferrite/martensite structure. Of these, ferrite/martensite solidification mode is classified another two kinds solidification as shown in Table 3.

Table 3. Transformation paths and Reaction

Transformation path	Reaction
Fully ferritic	L →L+F→F
Ferrite and martensite 1	L→L+F→F→F+A→F+M
Ferrite and martensite 2	L→L+F→L+F+A→F+A→F+M

Final condensation structure of fully ferrite structure exists in ferrite, and final structure of ferrite/martensite structure is the same ferrite/martensite in spite of different condensation process. Solidification mode is decided by carbon content. If carbon is 0.05 wt% ~0.15wt%, it progresses

Transformation path1. If over 0.15wt%, it conducts Transformation path2. Fig.3 shows a picture of microstructure according to Ti content. Fig.3 (a) is No. 1 specimen structure without Ti content, (b) is No. 2 specimen structure with 0.5% Ti, and (c) is No. 3 specimen structure with 0.8% Ti. From (a), we can see martensite formation in the shape of Widmanstatten side plate in ferrite grain boundary. If condensation starts from the area where kish ferrite and austenite liquid phase exist, then transformed into ferrite and austenite solid phase, and cooled, austenite will finally condensate into martensite. As carbon content of the specimen used in this study is 0.02%, it is considered Transformation path1 condensation mode. In Fig3. (b) and (c), all final condensation structures observed are ferrite structures, which is considered fully ferrite condensation mode. When the content of ferrite expansion element is higher than that of austenite expansion element, fully ferrite structure inhibits the transformation into austenite at high temperature to prevent martensite formation, according to the previous report.

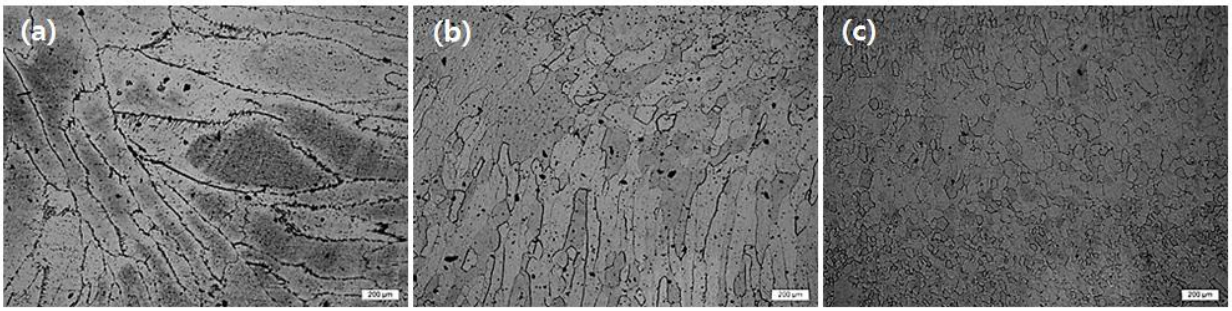

Figure 3. Microstructure of Weld metals : (a) No.1 (b) No.2 (c) No.3

Fig.4 shows the microstructure according to Ti content from the specimen heat treated for 2 hours at 850℃ after welding. Fig.4 (a) shows the picture of No. 1 specimen without Ti. We can see black precipitation along crystal grain boundary. EDS analysis in Fig.5 revealed that No. 1 specimen contained 47% chrome and 4% molybdenum. Precipitation of this composition is known as a sigma phase, which coincides with the study done by Esciba. [9-11] Kai phase also has chrome and molybdenum with the ratio of 2:1, but its precipitation temperature is lower than sigma phase.[12] we obtained the result that precipitation containing 42wt% chrome and 4wt% molybdenum coincided with sigma phase components in Zbigniwe study.[13] It is considered that No. 1 specimen used in this study created sigma phase along crystal boundary. We could observe that sigma phase was not precipitated when adding Ti; Ti(C,N) and chrome carbides were precipitated in the matrix through EDS and EBSD analysis.(fig.6) In general, it is reported that when 0.3-1.5wt% Ti is added, sigma phase precipitation is delayed. [8] The fact that Ti(C.N) was precipitated instead of sigma phase precipitation is because a ferrite expansion element Ti expands ferrite area and sigma phase lowers the temperature and inhibit the creation of precipitation. Besides, Ti precipitation formation energy is lower than Cr precipitation formation energy. [14] As a result, we could understand that the addition of stabilizing element Ti produces Ti precipitation in the grain and inhibits sigma phase formation.

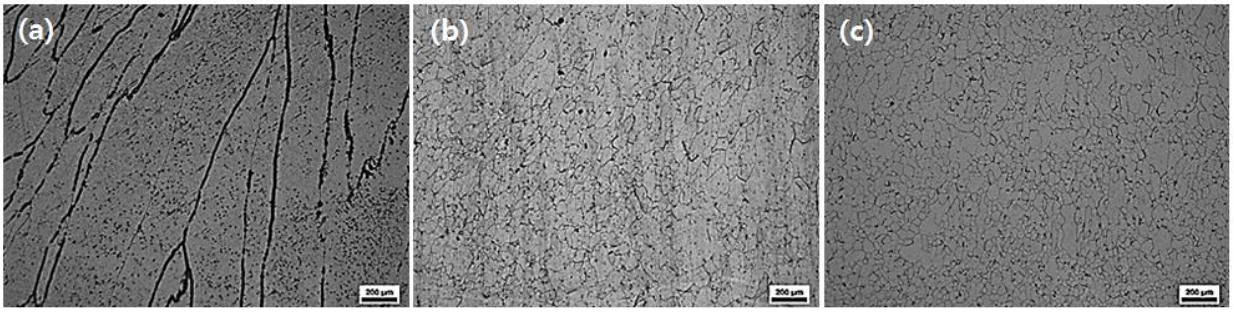

Figure 4. Microstructure of PWHT(Post Weld Heat Treatment) metals : (a) No.1 (b) No.2 (c) No.3

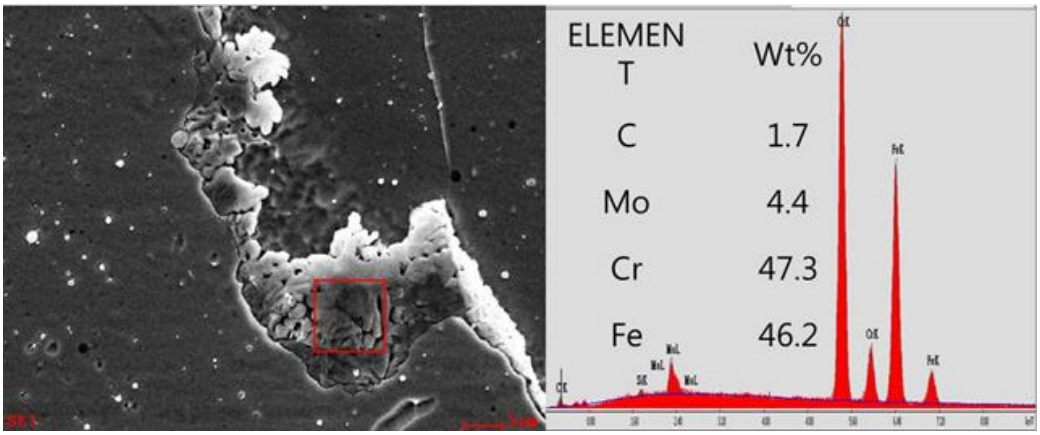

Figure 5. EDS of precipitation for the specimen aged at 850℃ for 2hr

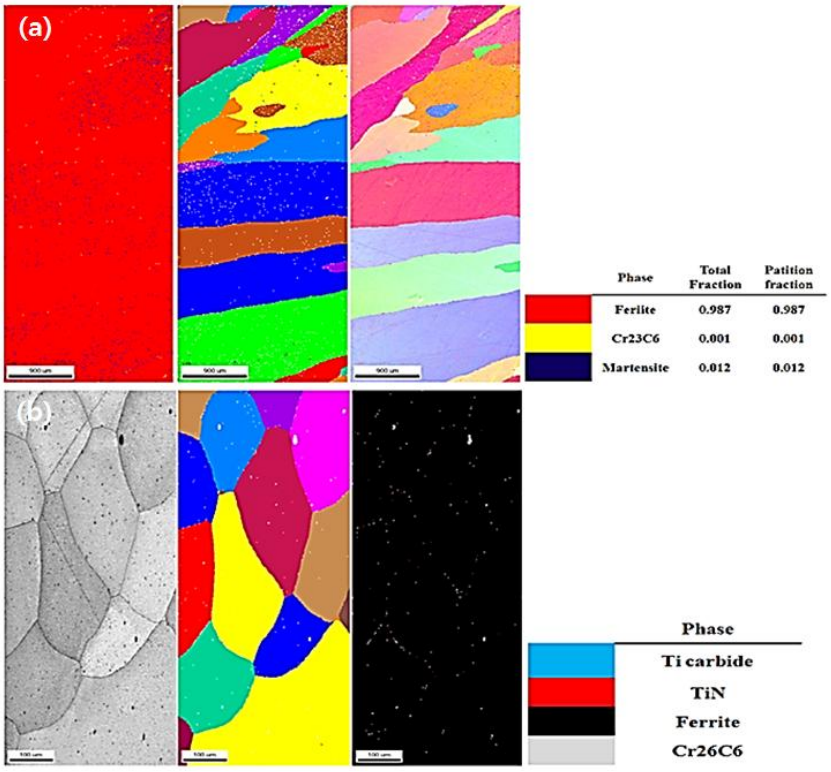

Figure 6. Result of the EBSD analysis (a) No.1 (b) No.2

3.2. Corrosion properties

Ti is known as an element to increase IGC (Intergranular Corrosion) resistance. To evaluate corrosion properties of ferrite stainless welding part according to Ti content, potentiodynamic polarization test was done in 3.5% NaCl solution, which is shown in Fig. 7. Its pitting mechanism is' $M^+Cl^-+H_2O \rightarrow MOH + H^+Cl$'. It acts as a catalyst for pitting, reacts with 'Cr^+ ion, destructs the passive film, and causes pitting corrosion.[1] In general, it indicated a curve type of ferrite stainless steel polarization, which started from the nearly same potential, since the passive film formation potentials made no difference, i.e., -0.3V for No. 1 specimen, -0.3V for No. 2 specimen, and -0.29V for No. 3 specimen. However, CPP (Critical pitting potential, Ep) increased with the addition of Ti content, and the passive range was expanded. Ep values were 0.2V, 0.4V, and 0.4V separately.

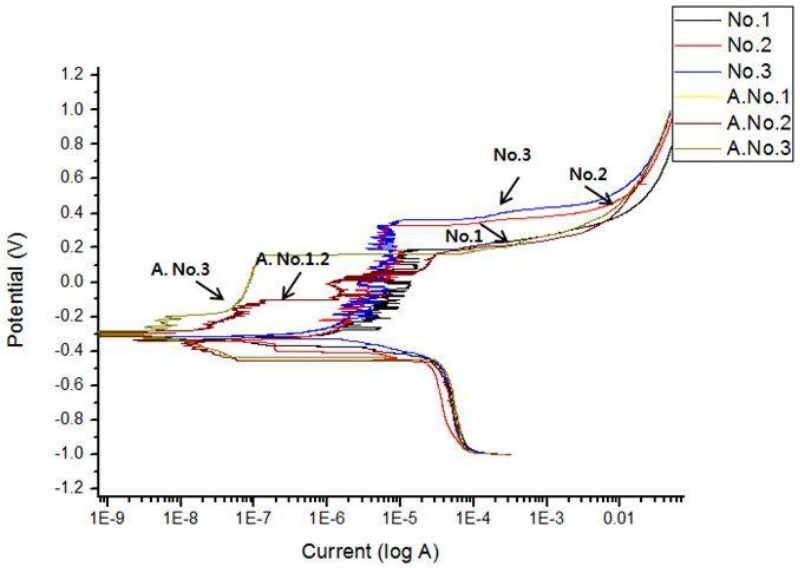

Figure 7. Potentiodynamic polarization curves of AISI 436 stainless steel weld metals in 3.5%NaCl

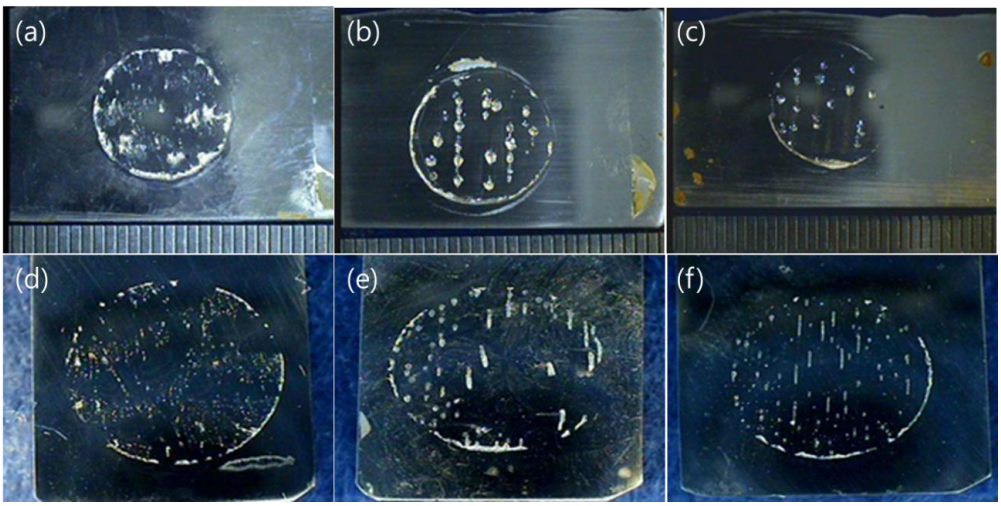

Figure 8. Macrostructure of weld metals after potentiodynamic polarization test: as weld (a) No.1 (b) No.2 (c) No.3 PWHT (d) No.1 (e) No.2 (f) No.3

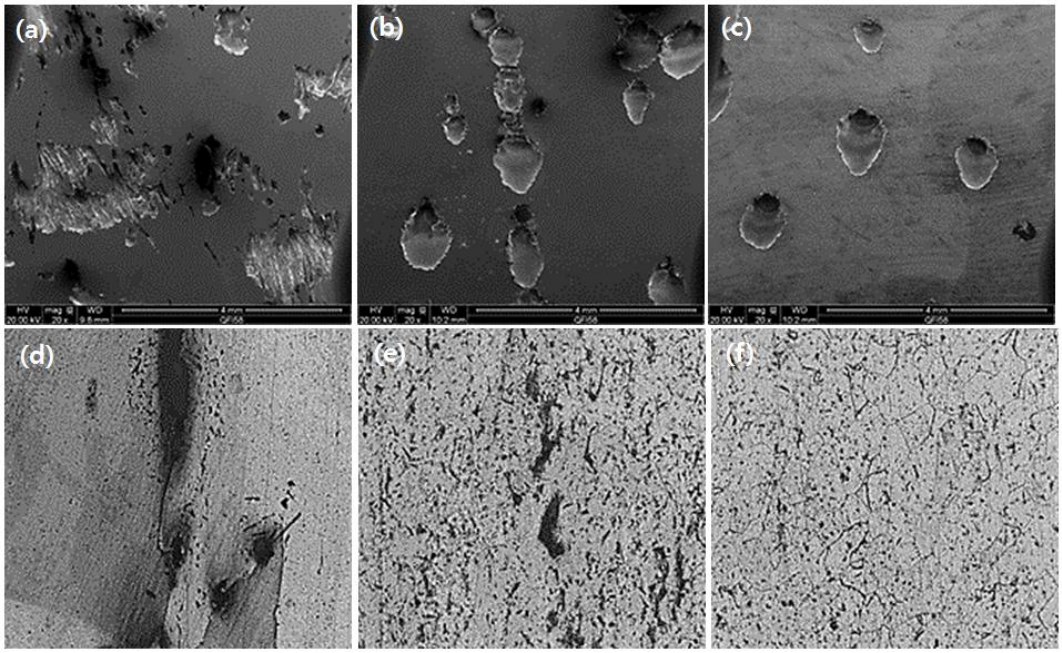

Figure 9. SEM images and Microstructures after potentiodynamic polarization test: AS weld (a) No.1 (b) No.2 (c) No.3 PWHT (d) No.1 (e) No.2 (f) No.3

Although CPP was measured high due to Ti addition, CPP did not increase with Ti addition. The amount of Ti addition for corrosion property improvement should be over 5 times of carbon content.[5] When Ti is added more than minimum content, it is considered that corrosion resistance effect is low in spite of the increased addition. It is known that the formation of sigma phase has an disadvantageous effect on pitting resistance and cavity corrosion, and intergranular corrosion occurs as chrome deficiency area forms around sigma phase. After executing potentiodynamic polarization curve test, in order to locate the creation of pitting, the test was stopped at the initial time of pitting creation. Then, we observed structures and SEM photos, and also macrostructures to see corrosive shape after potentiodynamic polarization test. As seen in Fig.8 and Fig.9, the specimen with no Ti proceeds to corrosion along the welding pass and corrosion starts from the crystal grain boundary. However, this tendency is not observed in the specimen with Ti. Corrosion started from inside the grain. We can see that as the addition increases, the degree of corrosion becomes smaller. No. 1 specimen with no Ti started to make pitting along the crystal grain boundary near the sigma phase precipitated in the grain boundary.

It is judged that No. 1 specimen made pitting due to the deficiency of Cr near the sigma phase. As seen in Fig. 10, EDS analysis of pitting of the specimen with Ti addition revealed that pitting started from Ti precipitation. Pitting occurrence of No. 2, 3 specimens with Ti addition showed the tendency to coincide the study done by 'Kim and Choi' that pitting occurs near Ti precipitation. [15,16] When we see that pitting, unlike No. 1 specimen, did not started from inside the crystal grain boundary, but started in the matrix for distribution, it is judged that Ti addition prevents intergranular corrosion to distribute pitting in the grain and to improve corrosion resistance. According to the observation of corrosion properties before and after heat treatment, heat treatment after welding

decreased the passive area and pitting potential, but its effect was very slight. It is considered that the corrosion resistance is decreased as the formation of Sigma phase due to the heat treatment. Also, the pitting potential of no.3 specimen is higher than that of the no.1 and no.2. This is because the precipitation of sigma phase was inhibited by the addition of titanium. As we see the increase of critical pitting potential and passive area in all specimens with Ti addition, it is judged that Ti addition prevents intergranular corrosion and improves corrosion resistance.

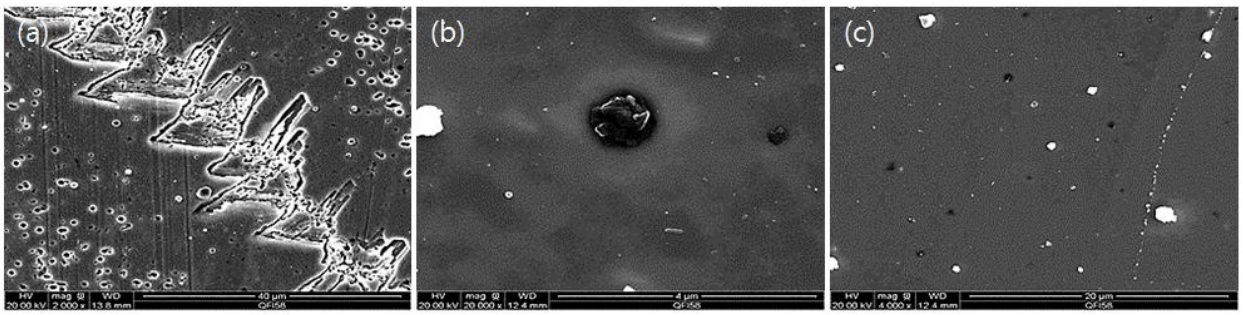

Figure 10. SEM images of weld metals after potentiodynamic polarization test: (a) No.1 (b) No.2 (c) No.3

4. CONCLUSIONS

With three kinds of welding wire having various Ti contents in AISI 436 stainless steel, the following conclusions were obtained by investigating microstructures and corrosion properties after FCA welding.

1. According to the observation on the microstructure, in the specimen with no Ti, martensite was formed, while in the specimen with Ti addition, martensite was not formed due to ferrite expansion effect. As Ti content increased, structure became finer.

2. According to potentiodynamic polarization test in 3.5% NaCl solution, passive formation potential was same. But, when Ti was added, passive area and pitting potential were increased.

3. Comparing No. 2 with No. 3 specimens all having Ti addition, in spite of higher Ti content of No. 3 specimen, there was no difference in pitting potential. That is because the addition more than the required amount of stabilizing element did not have a big influence on pitting potential.

4. As Ti addition increased, pitting potential difference became very slight. But, pitting size was reduced by addition of Ti.

ACKNOWLEDGEMENT
This investigation was supported by the Dong-A University Research Fund.

References

1. Nobuhiro Fujita, Keiichi Ohmura and Akio Yamamoto, *Mater. Sci. Eng*., A351 (2003) 272
2. S. G. Hong, H. S. Uhm and W. B. Lee, *Journal of KWJS*, 28 (2010) 12
3. S. G. Hong, M. H. Cho and K. B. Kang, *Journal of KWJS* 27 (2009) 72
4. J. Y. Song, I. S. Lee and Y. S. Ahn, *KSPSE* 14 (2010) 59
5. Cleiton C. Silva, Jesualdo P. Farias, Hélio C. Miranda, Rodrigo F. Guimarães, John W.A. Menezes and Moisés A.M. Neto, *Mater. Charact*. 59 (2008) 528
6. G. C. Lee, J. S. Kim, H. J. Kim, K. H. Lim and B. Y. Lee, *Journal of KWJS* 27 (2009) 145
7. Li-xin Wang, Chang-jiang Song, Feng-mei Sun, Li-juan Li and Qi-jie Zhai, *Mater. Des*, 30 (2009) 49
8. A. John Sediks, Corrosion of Stainless Steels. 2nd ed., Wiley, New York (1996)
9. A. Pardo, M.C. Merino, A.E. Coy, F. Viejo, M. Carboneras and R. Arrabal, *Acta Mater* 55 (2007) 2239
10. P. Muraleedharan, F. Schneider and K. Mummert, *J. Nucl. Mater*.270 (1999) 342
11. D.M. Escriba, E. Materna-Morris, R.L. Plaut and A.F. Padilha. *Mater. Charact*.60 (2009) 1214
12. S. B. Kim, K. W. Paik and Y. G. Kim, *Mater. Sci. Eng*., A 247 (1998) 67
13. Z. Stradomski and D. Dyja, Sigma phase precipitation in duplex phase stainless steels, in: Proceedings of 4th Youth Symposium on Experimental Solid Mechanics (2005)
14. T. J. Park, J. P. Kong, H. S. Na, C. Y. Kang, S. H. Uhm, J. K. Kim, I. S. Woo and J. S. Lee, *Journal of KWJS* 28 (2010) 320
15. H. S. Kim and D. Y. Choi, *J. Corros. Sci. Soc. of Korea* 29 (2000) 5
16. C.A.C. Sousa and S.E. Kuri, *Mater. Lett*. 25 (1995) 57